Helicopter Electromagnetic and Magnetic Surveys

By Bruce D. Smith, Robert R. McDougal, Maryla Deszcz-Pan, and Douglas B. Yager

Chapter E4 of
Integrated Investigations of Environmental Effects of Historical Mining in the Animas River Watershed, San Juan County, Colorado
Edited by Stanley E. Church, Paul von Guerard, and Susan E. Finger

Professional Paper 1651

U.S. Department of the Interior
U.S. Geological Survey

Contents

Plates

[Plates in this report are on accompanying CD-ROM]

Figures

Table

Chapter E4
Helicopter Electromagnetic and Magnetic Surveys

By Bruce D. Smith, Robert R. McDougal, Maryla Deszcz-Pan, and Douglas B. Yager

Abstract

A helicopter electromagnetic and magnetic survey over the Animas River watershed study area has greatly increased the resolution of airborne geophysical data for the study area. The main objective of this chapter is to present geophysical data and maps that can be compared to other data sets and maps of the study area. The results of the survey are useful in mapping surface and subsurface lithology and structure. A brief discussion of selected geophysical anomalies and trends is given. The total-field magnetic and apparent conductivity maps from the helicopter survey are used to interpret near-surface and deep geologic and hydrologic features that can influence ground-water flow. This qualitative discussion supplements a more detailed study using quantitative predictive modeling to characterize structures in the study area.

The total-field reduced-to-pole magnetic map is given at a scale of 1:48,000 superimposed on a topographic base. Derivative maps are given in color shaded relief at a scale of 1:100,000 and include high- and low-pass filtered maps. Qualitatively, a central magnetic low with peripheral magnetic highs caused by younger intrusives characterizes the Silverton caldera. Magnetic lows may be associated with alteration that has destroyed magnetic minerals and (or) may be associated with reverse magnetization.

Helicopter-borne measurements from five frequencies and two system geometries were used to compute apparent electrical conductivities. The pre-processed electromagnetic data have high noise along flightlines due to helicopter flying limitations caused by the high rugged terrain. The apparent conductivity map for the intermediate frequency (and depth of investigation) is given at 1:48,000 and again on a topographic base. The apparent conductivity is also presented as color shaded-relief maps at a scale of 1:100,000 for three frequencies and one system configuration. These maps reflect variations of the subsurface electrical conductivity ranging in depth from a few meters to on the order of 60 meters. The Silverton caldera is generally characterized by conductivity lows in the central part ringed by conductivity highs. Conductivity highs can be related to electrically conductive surficial rocks and sediments as well as deeper bedrock alteration both in narrow zones along drainages and in broad areas of hydrothermal alteration.

High apparent conductivities near one mine-waste pile suggest near-surface flow paths and a source for high dissolved solids where high-sulfide mill tailings have been removed after the helicopter survey. The youngest dacite-rhyolite intrusives show different types of magnetic and electrical properties that may be associated with different types of lithologic and ground-water regimes. Apparent conductivity maps suggest a northwest-trending structural zone along Cement Creek and extending toward Ohio Peak that may influence ground-water flow.

Introduction

An airborne electromagnetic and magnetic survey was flown over portions of the Animas River watershed to supplement other geologic, geochemical, and hydrologic studies that were carried out for the collaborative study. New airborne geophysical data were needed because the only available data for the study area were total-field magnetic and radiometric data with a flightline spacing of 2 miles (Oshetsky and Kucks, 2000). In general airborne geophysical methods provide data to interpret subsurface lithology, structure, and in some cases electrically conductive ground water. Smith and others (2000) have described how airborne geophysical surveys can be applied to abandoned mine land studies. McCafferty and others (2004) have demonstrated the application of quantitative class modeling of airborne electromagnetic and magnetic survey data in predictive mapping of acid-neutralizing terrains in the Boulder River watershed, Montana.

One main focus of the Animas River watershed AML study has been the source, transport, and fate of acid water derived from mining activities and from areas that have not been mined. Though much of the ground-water flow is through streams, an unknown amount flows through the subsurface colluvium and bedrock of the study area. Little specific information about the nature of this subsurface flow exists, although Huntley (1979) and Caine (2003) have made some generalizations on a watershed scale. Ground and airborne geophysical studies provide data that can be used to interpret subsurface heterogeneities that can be related to the origin and flow of acid water.

Purpose and Scope

The purpose of this investigation is to present the results of a helicopter electromagnetic and magnetic (HEM) survey flown over the Animas River watershed study area. The results of the survey are useful in mapping surface and subsurface lithology and structure. Geophysical maps from the airborne geophysical surveys are given in plates 3 and 4 of this volume. The objectives of the study are to:

- Present the airborne geophysical data in maps that can be compared to other maps from the AML study
- Describe data collection and reduction procedures for the airborne survey
- Present derivative maps that can be used in interpretation of subsurface geophysical features
- Provide some interpretation of geophysical anomalies in terms of lithology, structure, and possible hydraulic features.

Geophysical Surveys

A regional airborne survey of the study area was flown as part of the National Uranium Resource Evaluation (NURE) with E.-W. flightlines 400 feet[1] above ground with 2 mile spacing (Aero Service, 1979). Oshetsky and Kucks (2000) used these data and other airborne surveys to compile a statewide total magnetic field grid at 1,000 feet above ground level with a cell size of 500 m square. Figure 1 shows a portion of this regional airborne magnetic map for the northwestern part of the San Juan volcanic field with the main drainages of the Animas River watershed study area (from west to east, Mineral Creek, Cement Creek, and Animas River). Locations of three detailed helicopter geophysical surveys that have been flown in the Silverton and Lake City caldera areas are shown as boxes in figure 1 and in figure 2 with more detail. The detailed surveys are located over the Lake City caldera (Red Cloud and Lake City surveys in fig. 2, not discussed here) and the Silverton caldera (Animas survey in fig. 2; see following discussion). The regional airborne magnetic survey shows that the Lake City caldera is generally characterized by magnetic highs, in contrast to the older Silverton caldera, which is characterized by a central magnetic low. Grauch (1987a) observed that the magnetic expression of the Silverton Volcanics (postcaldera volcanic flows and volcaniclastic sediments) is low within the Silverton caldera and high within the Lake City caldera. The contrasting magnetic expression within this unit is due to variable natural remanent magnetization and to alteration.

[1]Measurements originally made and reported in feet and miles are retained here in their original units for clarity and to avoid misstatement of precision in conversion. To convert feet to meters, multiply by 0.3048; to convert miles to kilometers, multiply by 1.61.

The Red Cloud survey (fig. 2) was flown as part of the NURE program (High Life Helicopters, 1983) with N.–S. lines spaced 0.25 mi (miles) using spectral radiometric and total-field magnetic systems. The Lake City helicopter survey flown (fig. 2) as part of USGS programs (High Life Helicopters, 1981) used 0.3 mi flightline spacing, N.–S. lines, 400 ft above ground. Grauch (1987a, b) has interpreted the Lake City survey with emphasis on effects of the rugged terrain on the magnetic data.

The Animas helicopter electromagnetic and magnetic (HEM) survey was conducted over part of the Animas River watershed (fig. 3) during late May 1999 (Smith and others, 2000, 2004) under a contract to the U.S. Geological Survey. The objective of this survey was to map subsurface lithology and structure that could be important in geologic, structural, and hydrologic studies related to the Animas River AML study. The survey flightline spacing was 200 m and 400 m, as shown in figure 3. Closer flightline spacing was used in the western part of the survey area in order to improve resolution in the area of Mineral and Cement Creeks. In addition, flightlines were flown along South Fork Mineral Creek, Mineral Creek, Cement Creek, and the upper Animas River. These flightlines were done to obtain more detailed data along the drainages where tracer studies were planned (Kimball and others, this volume, Chapter E9). They were flown at a more constant elevation than was possible with the north-south flightlines. The stream valleys are deep and narrow, which makes it difficult for a helicopter to maintain constant elevation when crossing the terrain. Four east-west flightlines were flown as tie lines for processing the magnetic field measurements.

The nominal helicopter flight height was specified to be 60 m above terrain. In practice the flight elevation varied between 60 and 90 m due to flight safety considerations in the extremely rugged terrain. The geophysical electromagnetic (EM) and magnetic system was towed in an 8 m long torpedo-shaped “bird” at a distance of about 30 m below the helicopter. The instrumentation included a high-precision GPS system that provided a positional accuracy of about 5 m. Barometric and radar altimeters provided additional data on the elevation. The position of the flight path provided by the GPS was checked with video records from the flight path video camera.

Magnetic System and Data Processing

A cesium split-beam total-field magnetic sensor was used for the magnetic field measurements. The in-flight sensitivity of the system was 0.001 nanotesla (nT) with a recording rate of 0.1 second. The sensor tolerated gradients up to 10,000 nT/m, and the dynamic range was 20,000 to 100,000 nT. A heading test after system installation and prior to surveying showed a maximum variation of ±0.92 nT. A total-field magnetic base station placed within the survey area used a sensor with the same specifications as the airborne sensor. No magnetic storms occurred during the survey.

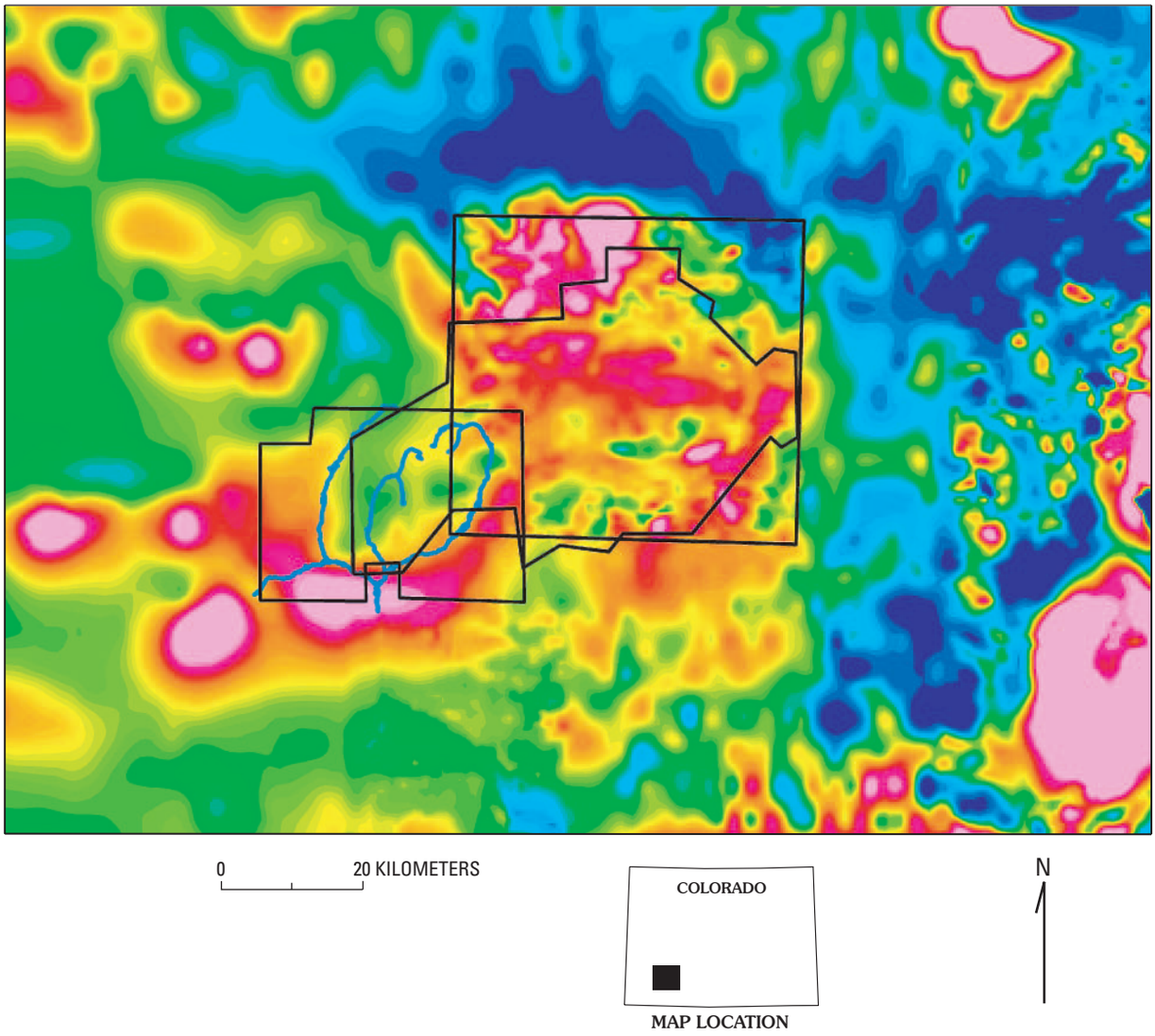

Figure 1. Total-field magnetic map of a region surrounding the Animas River watershed study area. Data are a subset from the compilation of Colorado aeromagnetic data by Oshetski and Kucks (2000). Warmer colors (reds), magnetic highs; cooler colors (blues), lows. The digital grid has a cell size of 500 m square. Boxes indicate areas where detailed helicopter surveys were done (see fig. 2 for scale). Blue lines, main drainages of the study area (see fig. 3), from west to east, South Fork Mineral Creek, Mineral Creek, Cement Creek, and Animas River.

The in-flight magnetic field data were corrected for diurnal variations using the base station records. The International Geomagnetic Reference Field (IGRF) was computed and removed along each flightline. The magnetic data were gridded using minimum curvature methods with a 40 m square cell size for the western part of the survey area and an 80 m cell size for the eastern part of the survey (fig. 1). The eastern grid was resampled to a 40 m cell size and merged with the western grid.

The IGRF-corrected total-field magnetic grid was filtered using a reduction-to-pole (RTP) filter implemented in the USGS potential field programs (Phillips, 1997; Phillips and others, 2003). This filter transforms the magnetic field so that anomalies are positioned directly above the causative body. This filtering will produce a correct positioning of the magnetic responses as long as (1) the causative source of the magnetic anomaly does not have a strong natural remanent magnetization and (2) the magnetization is predominantly all induced in the direction of the current main magnetic field. Although some rock units in the Silverton caldera exhibit remanent magnetization (Grauch and Hudson, 1987), the magnetization intensities and directions are low and within a range collinear with the present-day magnetic field.

The RTP magnetic grid was also filtered to separate short and long spatial wavelengths through a process termed matched filtering (Syberg, 1972). USGS computer field programs by Phillips (1997) were used to do this processing. The short wavelength anomalies approximate sources that are

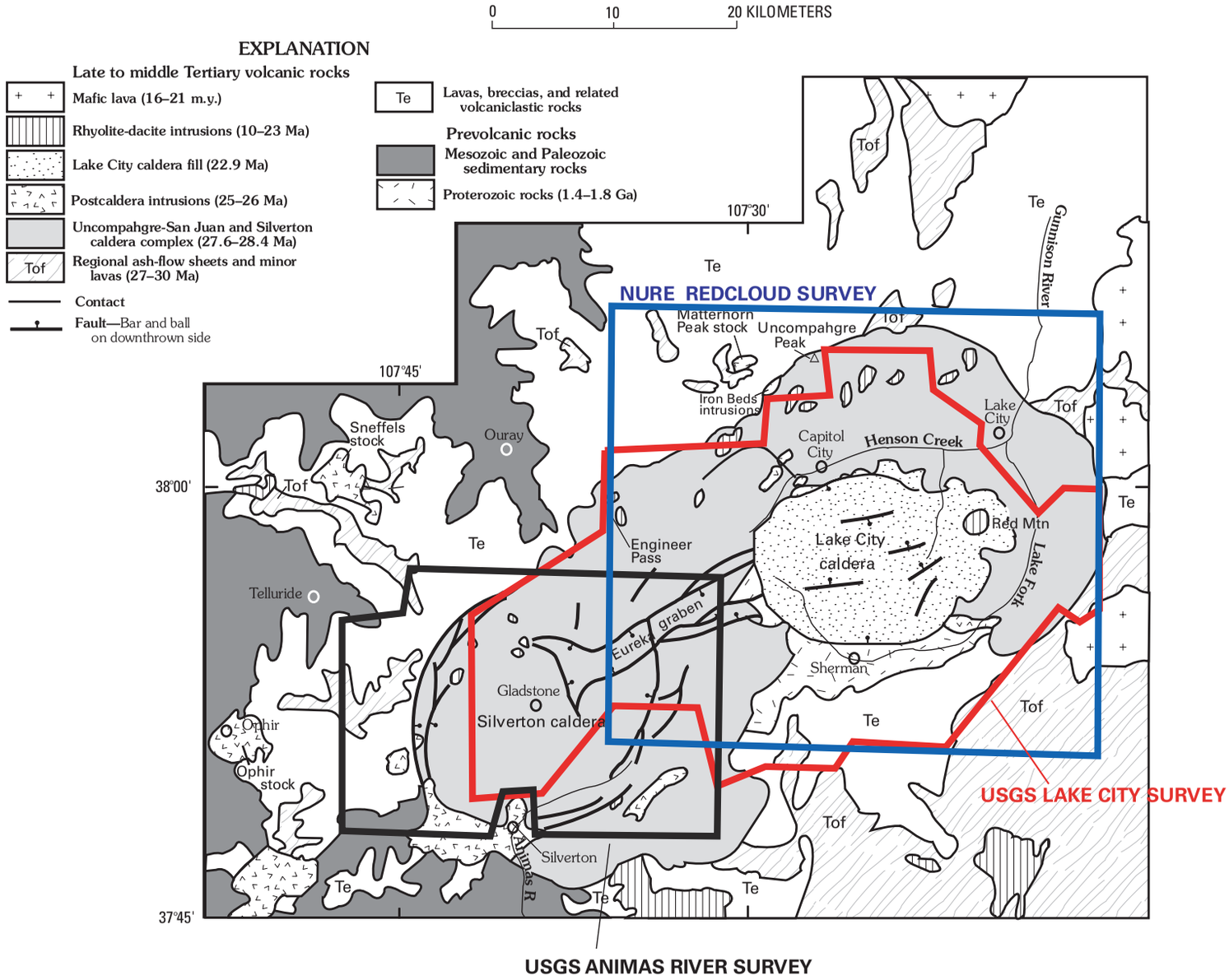

Figure 2. Generalized regional geology of Silverton and Lake City calderas, southwest Colorado. Heavy solid line, boundary of detailed aeromagnetic surveys flown in area. Magnetic maps from USGS Animas survey are discussed here. Geologic index map modified from Bove and others (2001). Geologic map for the Animas survey area is in Yager and Bove (2002) and plate 1 of this volume.

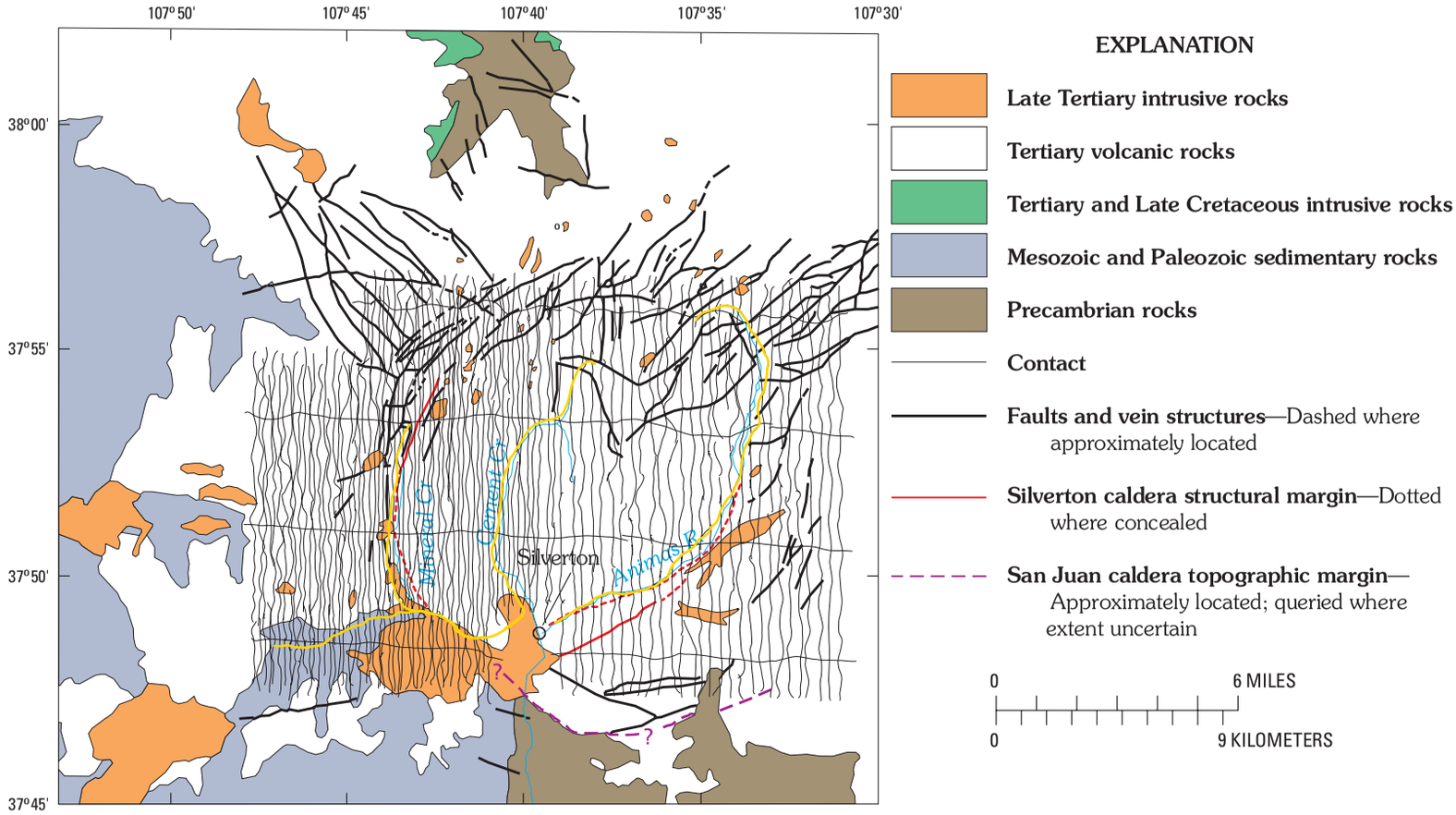

Figure 3. Generalized geology of Animas River watershed study area, southwest Colorado. Thin north-south black lines, flight path of helicopter in main part of survey area. East-west lines, tie lines. Yellow lines are flightlines flown along selected drainages. Major tributaries to the Animas River are shown in addition to major Tertiary volcano-tectonic structures related to the Silverton and San Juan calderas. Figure is modified from Casadevall and Ohmoto (1977).

in the upper 200 m beneath the topographic surface. The map produced from this data is termed a "high-pass" magnetic anomaly map and should correspond most closely with the sources of anomalies from the electromagnetic survey.

A matched filter was also applied, using the same programs (Phillips, 1997; Phillips and others, 2003), to enhance long wavelength anomalies that could represent sources at depths of more than 1,300 m. This map is termed a "low-pass" magnetic anomaly map.

Electromagnetic System and Data Processing

The EM system consisted of five coil pairs operating at different frequencies. Three of the coil pairs were oriented in a horizontal coplanar (CPL) configuration and the other two in a vertical coaxial (CXL) configuration. Table 1 gives the frequencies for each of the coil configurations. The frequencies were set before the survey was started and were maintained during flight operations.

Data from the CXL configuration, normally used in exploration for dike-like conductors, are very susceptible to in-flight noise and have not been used in this study. The CPL coil pairs are best suited to mapping of subsurface electrical conductivities.

Care was taken to establish calibration levels for the electromagnetic system both before and during the survey. However, in post-processing by the USGS, absolute levels of the EM channels were found to be unreliable. A number of different approaches (Fitterman, 1999) were used to adjust the levels to produce agreement with ground electromagnetic measurements. None of these methods could entirely correct the data. The data presented here have not been adjusted beyond the leveling done by the contractor who conducted the airborne survey. Quantitative interpretations beyond the qualitative interpretation presented here will require additional leveling of the HEM survey data.

The contractor used the EM measurements at each frequency to calculate apparent resistivity using the method described by Fraser (1978). The method estimates the resistivity of a homogeneous half space based on the EM measurements, hence the term apparent resistivity. For the purposes of this study, the apparent resistivity (ρ, ohm meters) was converted to apparent conductivity (σ, millisiemens per meter) where $\sigma=1{,}000/\rho$. Maps of apparent conductivity presented here show high conductivities in warmer colors in order to emphasize such features.

Table 1. Frequency and coil orientation for the electromagnetic system.

Frequency (Hz)	Configuration
886.00	Coaxial
984.00	Coplanar
4,836.00	Coaxial
4,310.00	Coplanar
32,960.00	Coplanar

Map Compilation

The digital raster graphic topographic base map was scanned from a green-line topographic base. The base is the same digital map as used for the geologic map of the Animas River watershed study area and vicinity (Yager and Bove, 2002, and Yager and Bove, this volume, Chapter E1, pl. 1). All of the digital data were projected to the Universal Transverse Mercator (UTM zone 13) geographic projection. The digital database used a 2.5 m resolution and was resampled to 8 m for the digital version of the base. All of the airborne geophysical data used this same projection. The positional accuracy of the HEM survey is on the order of 5 m in the horizontal position and 10 m in the vertical position based on the post-processing of the differential global positioning system (GPS).

Magnetic and Electrical Properties

Magnetic Responses

The magnetic response of the volcanic rocks is controlled by the amount of magnetic minerals, primarily magnetite and to some degree ilmenite, maghemite, and titanomagnetite present in the rocks (Telford and others, 1978). Pyrrhotite is a magnetic iron sulfide mineral that is common in some sulfide mineral deposits but does not occur in abundance in the mineralized systems in the study area. The amount of magnetic minerals in rocks determines the magnetic susceptibility and thus its strength of magnetization. Rocks with a high susceptibility will produce a strong dipolar magnetic response (Telford and others, 1978). Natural remanent magnetization (NRM) also affects the amplitude of observed magnetic anomalies depending on its direction and intensity. Often the direction of the NRM is opposite that of the induced magnetization, resulting in a lowering of magnetic response or reversal of the dipolar signature. Grauch and Hudson (1987) and Gettings and others (1994) have examined the NRM and magnetic susceptibility of the volcanic rocks in the Silverton and Lake City calderas. The nature of NRM has been discussed previously in regard to processing of the total-field magnetic data. As is typical of many volcanic terrains, both NRM and magnetic susceptibility are highly variable both within and between stratigraphic and lithologic units. Basic igneous rocks have high magnetization, with granite, andesite, and rhyolite having generally lower magnetization. Volcanic rocks in general have higher magnetization than sediments unless the sediments contain magnetite. Hydrothermal alteration of volcanic rocks is likely to reduce their magnetite content (Telford and others, 1978). Several different types of alteration have been observed and mapped in the study area (Bove and others, 2000; McDougal and others, this volume, Chapter E13).

Electromagnetic Responses

Several factors control the electrical conductivity of rocks (Telford and others, 1978; Olhoeft, 1985), and these can be generalized for the geologic setting of the study area. In general, introduction of clay minerals (including zeolites) tends to increase the electrical conductivity of rocks. Both hydrothermal alteration and weathering processes of volcanic rocks in the area can produce clay minerals. Metallic veins, particularly massive sulfides such as pyrite, can drastically increase the electrical conductivity. Ground water having high dissolved solids can increase measured electrical conductivity. Sediments in valley fill may be much more conductive than bedrock due to silt (particularly with high organics) and clay mineral content and water with high dissolved solids. However, the processes that create valley fill may also weather the bedrock under the valleys, reducing the electrical contrast between rock units. Some types of glacial sediments, such as moraines, may have high clay content and thus high electrical conductivity.

Areas of low conductivity (high resistivity) can be caused by alteration that causes silicification of porous media. McDougal and others (this volume) have analyzed the electromagnetic data to map areas of low conductivity that may be associated with fracture and fault systems. In general, any process that decreases the permeability and porosity of rocks tends to increase the resistivity or lower the conductivity. This variation is related to observation that the amount and nature of pore fluids have an enormous effect on the electrical resistivity of rocks (Olhoeft, 1985). Thus rocks above the water table generally have a low conductivity.

Discussion

Geophysical maps from the helicopter magnetic (pl. 3) and electromagnetic (pl. 4) survey are given at scales (1:48,000) comparable with the geologic map of the study area (Yager and Bove, 2002, and pl. 1, this volume). The purpose of the following section is to illustrate interpretations of specific anomalous features that are relevant to the Animas River watershed AML study. A detailed discussion of the airborne geophysical data is given by McDougal and others (this volume) in terms of quantitative predictive modeling designed to characterize structural and lithologic terrains.

Magnetic Maps

Plate 3 gives the color total-field magnetic map for the Animas River watershed study area superimposed on a topographic base. The 1:48,000-scale total-field reduced-to-pole (see processing section) magnetic map can be compared directly to the geologic map of the study area given by Yager and Bove (2002, and this volume, pl. 1). The color shaded-relief map is shown for the total-field magnetic survey data in figure 4. The shading is shown with a sun angle from N. 45° E., which emphasizes trends in the conjugate (N. 45° W.) direction.

The reduced-to-pole map (pl. 3 and fig. 4) generally shows that the central part of the Silverton caldera is defined by magnetic lows relative to the margins. The high-pass magnetic map (fig. 5) shows features that should be from sources at depths similar to the EM data. The low-pass magnetic map (fig. 6) shows longer wavelength magnetic responses that are caused by sources that are deep or broad and shallow. Specific features of each map are discussed in following paragraphs and also by McDougal and others (this volume).

Magnetic Features

Magnetic features are shown in figure 7, where letters identify linear features and numbers identify anomalies. Anomaly 10 in figure 7 is a discrete magnetic low. Narrow high magnetic anomalies that occur in the east and north part of anomaly 10 may be dikes. The magnetic low may extend farther to the east beyond the dikes. Rocks that are either reversely polarized or intensely altered (where the magnetic minerals have been destroyed) are possible sources for the magnetic low.

Linear feature P (fig. 7) is located on the southeast of magnetic anomaly 10. Interpreted linear features Q, R, and S in the magnetic map (fig. 7) may indicate structures that cross the caldera boundaries. Such structures could influence ground-water flow directions in the caldera ring fault system.

The magnetic high anomalies labeled 15 (fig. 7) are associated with the Sultan Mountain stock (Yager and Bove, 2002; this volume, pl. 1), one of the Tertiary intrusives in the San Juan caldera complex. The strong magnetization suggests that this late Tertiary intrusive complex is unaltered.

The area of peak 3,792 m, between Middle and South Forks Mineral Creek (Yager and Bove, this volume; Bove and others, this volume), is characterized by a magnetic high (anomaly 16, fig. 7). The magnetization is not as intense as the magnetization of the Sultan Mountain stock.

Magnetic high anomalies occurring at the south edge of the Silverton caldera are labeled 11 (fig. 7). The magnetic highs correlate with topographic highs and are likely due to the relatively flat lying Henson Member of the Silverton Volcanics. The magnetic rocks of the Sultan Mountain stock have been mapped just north of the Animas River; so some of the high magnetic anomalies just to the northwest of the junction of the Animas River and Cement Creek may be due to this source.

Several small isolated magnetic high anomalies are labeled 12 in figure 7. Farther east, in the Lake City caldera, this type of magnetic anomaly is associated with late Tertiary intrusives, which have been discussed in detail by Bove and others (2001). Anomaly 13 (fig. 7) is a magnetic low in the upper Animas River basin. This magnetic low is not associated with nonmagnetic valley fill, but is more likely caused by volcanics that have very little magnetite (perhaps due to alteration) or are reversely polarized.

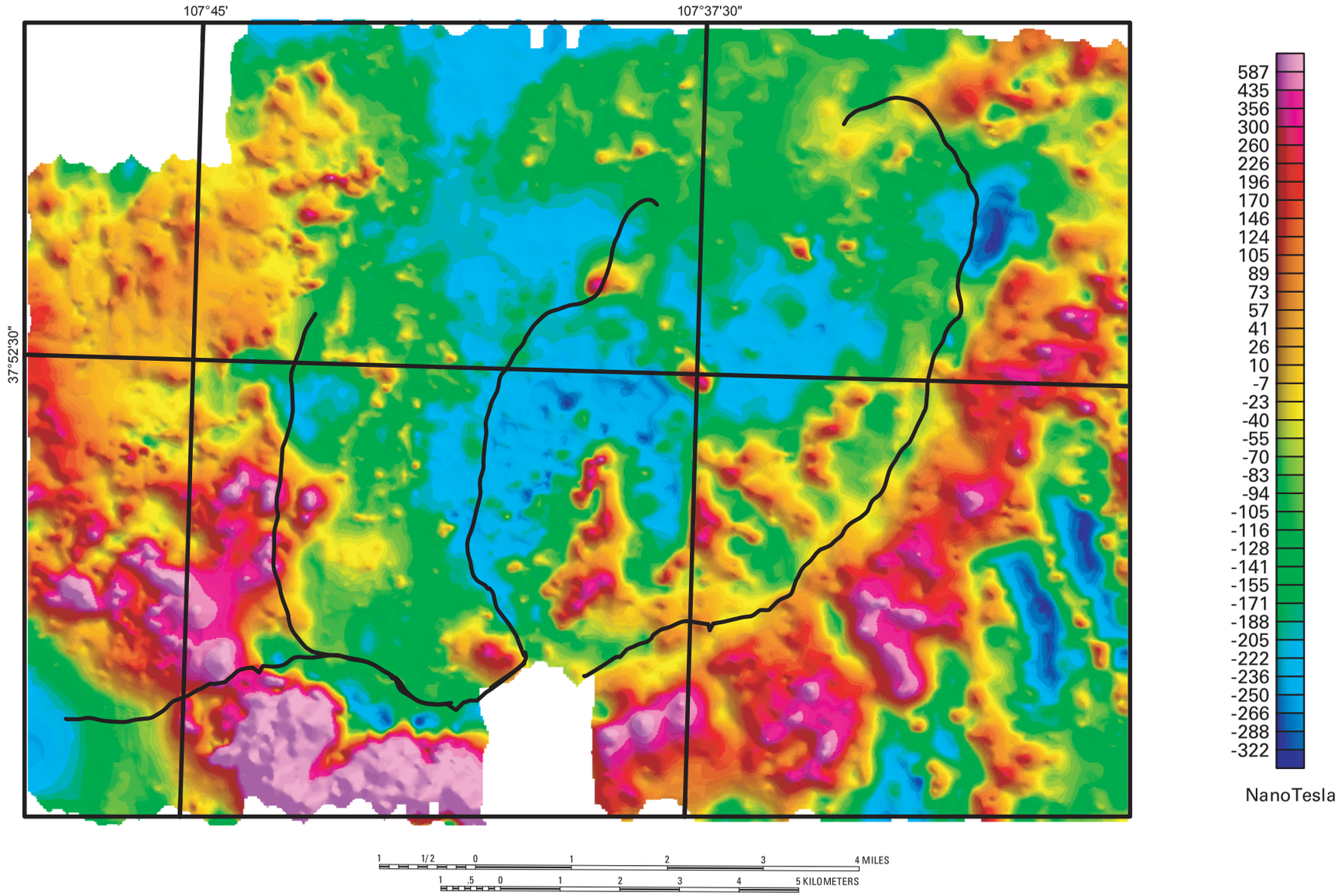

Figure 4. Color shaded-relief reduced-to-pole total-field magnetic map of Animas River watershed study area. Color scale bar shown at right. Sun direction is from northeast. Black line, flightline flown along selected drainage as shown in figure 3. Figure is of same area as shown in the 1:48,000 reduced-to-pole magnetic map (pl. 3).

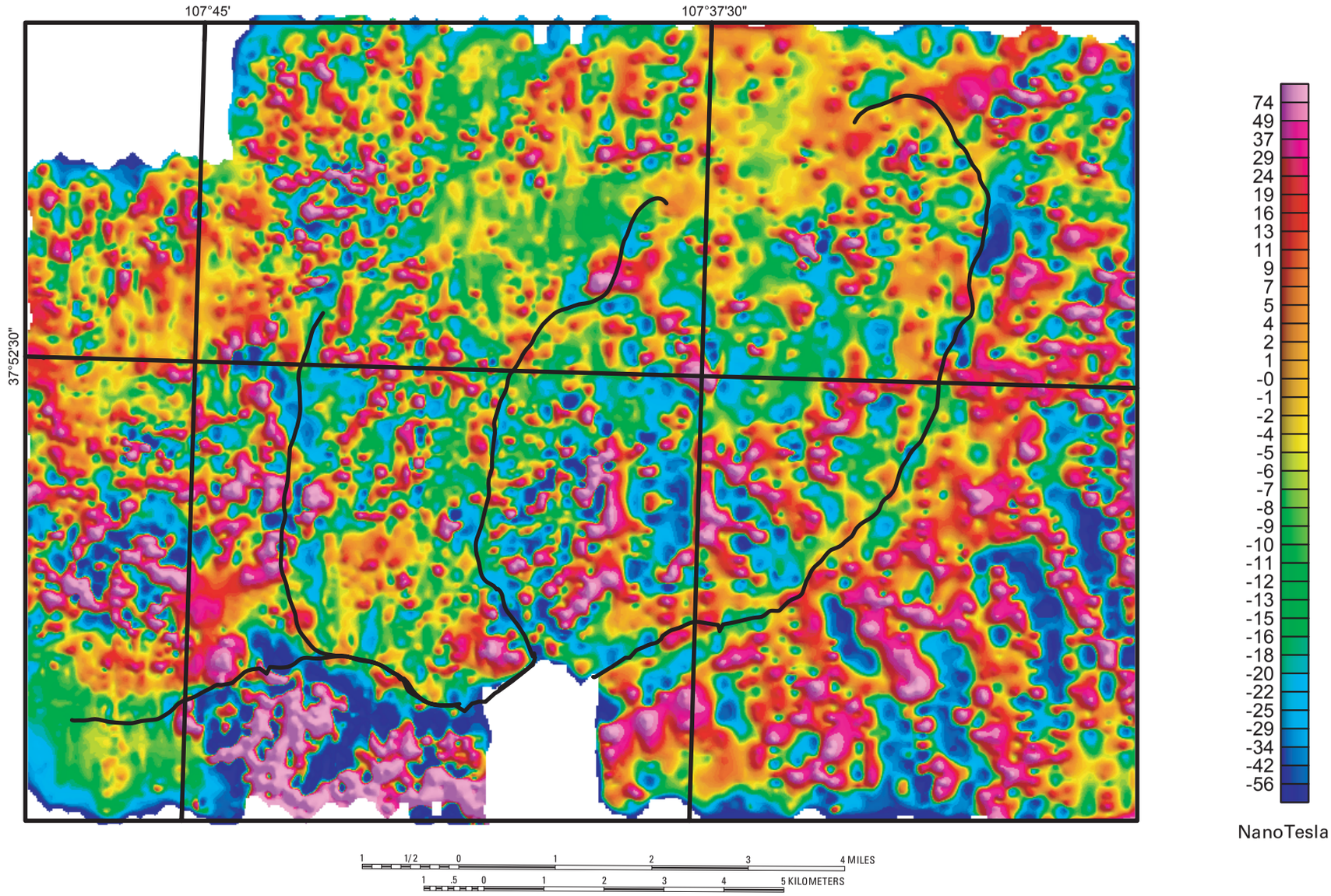

Figure 5. Color shaded-relief high-pass filtered RTP map for Animas River watershed study area. Sun direction is from northeast. Black line, flightline flown along selected drainage as shown in figure 3. Figure is of same area as shown in the 1:48,000 reduced-to-pole magnetic map (pl. 3).

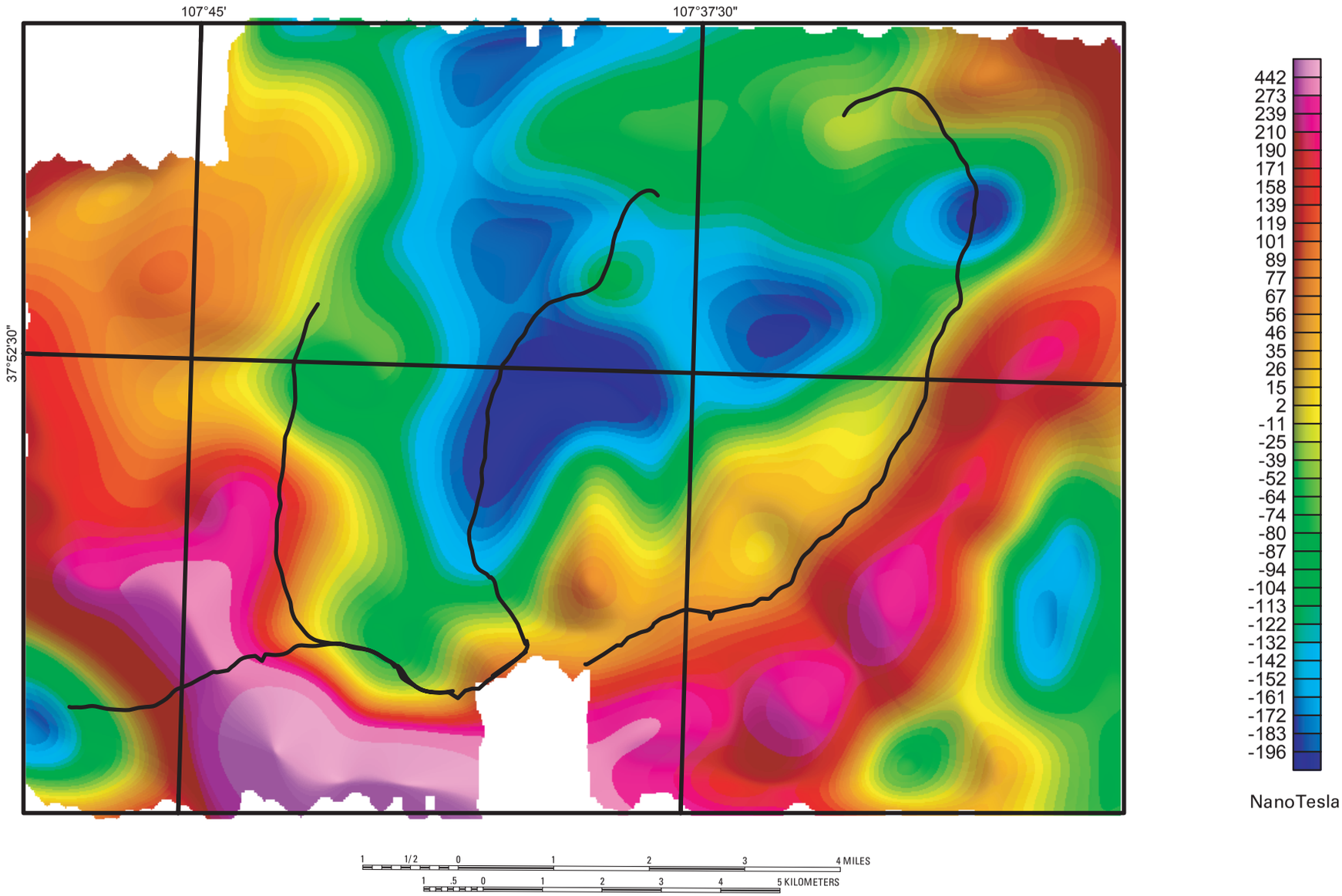

Figure 6. Color shaded-relief low-pass filtered RTP map for Animas River watershed study area. Sun direction is from northeast. Black line, flightline flown along selected drainage as shown in figure 3. Figure is of same area as shown in the 1:48,000 reduced-to-pole magnetic map (pl. 3).

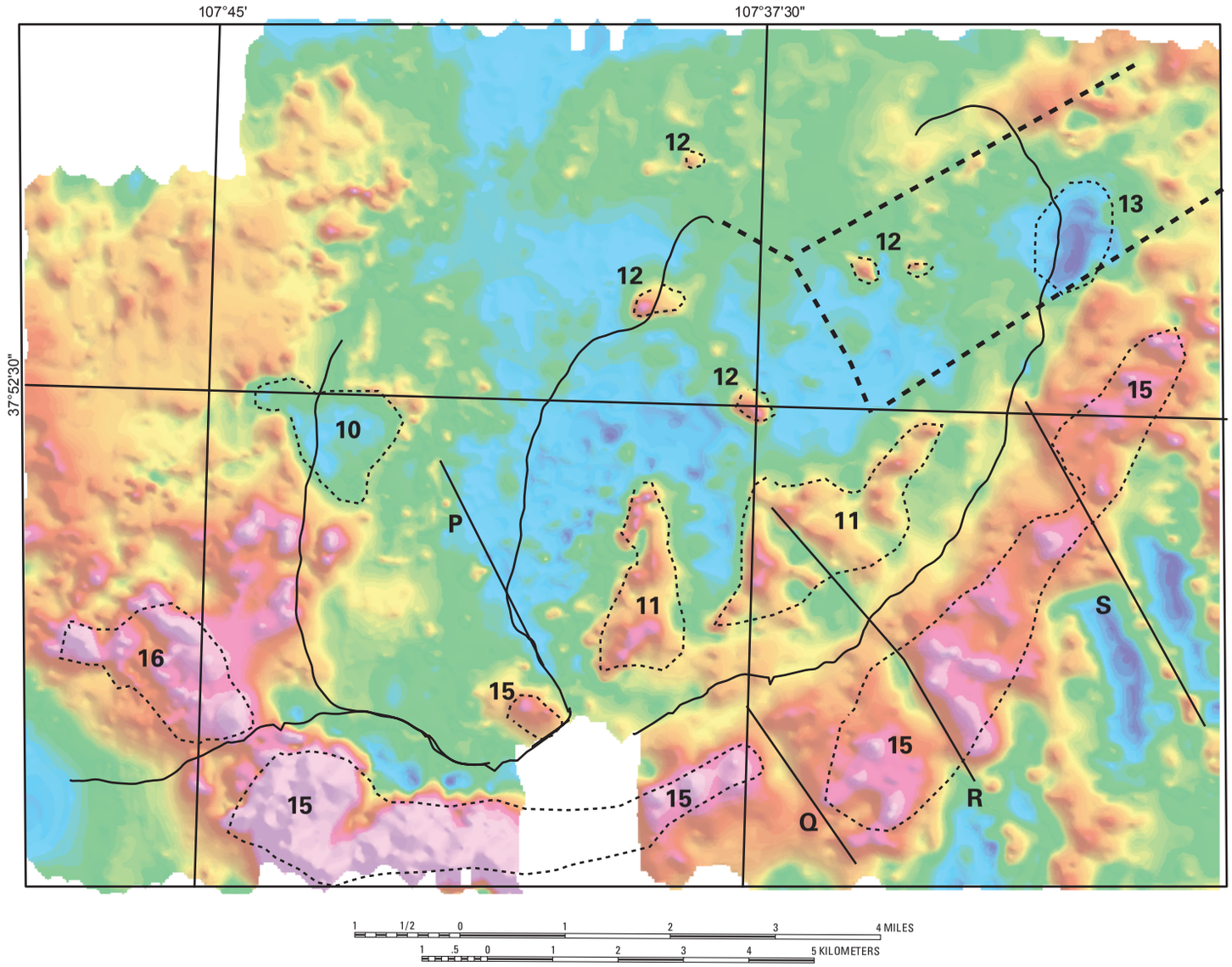

Figure 7. RTP magnetic map showing selected anomalous features. Linear features (bold letters and black lines) are selected from a number of features identified by McDougal and others (this volume). Magnetic anomalies (numbers) have been selected to characterize general geologic features. Color shaded relief from figure 4 is shown as background. Curving solid black line, flightline along selected drainage. Heavy dashed line is general outline of Eureka graben.

Apparent Conductivity Maps

Plate 4 shows apparent conductivity in the Animas River watershed study area. The 1:48,000-scale color apparent conductivity map can be compared directly to geologic maps of the study area (Yager and Bove, 2002; Yager and Bove, this volume, pl. 1). The intermediate frequency (4,310 Hz) has been used for the main map because it best represents general characteristics of the electrical structure of the study area.

Color shaded-relief (CSR) maps are commonly used to emphasize trends. Figures 8–10 show CSR maps of apparent conductivity for the three horizontal coplanar coil pairs from high to low frequency. The sun illumination angle is N. 45° E. with an inclination of 45°. Thus, features trending northwest are emphasized. In these maps, the high conductivities are shown in warm colors (reds) that correspond to low resistivities. The general structural trends described by Burbank and Luedke (1969) are northeast, north, and northwest. Maps using several different illumination angles were examined, and the northeast illumination direction was qualitatively the best to emphasize trends discussed herein. However, this illumination angle does not emphasize the northeast-trending structures described by Casadevall and Ohmoto (1977), such as the Eureka graben. The use of particular color scales (resistivity or conductivity) depends on the type of geophysical features that are being highlighted. In this discussion, conductive features are highlighted using warmer colors. The color scale for each frequency is stretched to yield a consistent scale between maximum and minimum values of apparent conductivity. Note that this results in specific colors on each map representing different apparent conductivity.

The highest frequency (fig. 8) has the greatest spatial frequency variation due to more system noise from in-flight altitude variations and also due to large variations in shallow geology. At this frequency, the depth of investigation is only a few meters. Areas of high anomalous conductivity (fig. 8) are generally located in the northwest, between Cement and Mineral Creeks, and in the area of peak 3,792 m. The south end of the Eureka graben (fig. 3) is associated with a shallow high conductivity anomaly (fig. 8). A high conductivity anomaly also lies along the northern part of the Animas River.

The intermediate-frequency apparent conductivity map (fig. 9) has less high spatial frequency variations due to less system noise, greater spatial averaging, and deeper penetration. The depth of penetration at this frequency is on the order of 30–40 m. High apparent conductivities (fig. 9) are generally in the same areas as for the higher frequency (fig. 8). One difference between figures 8 and 9 is that high apparent conductivities occur along a longer part of the Animas River at the intermediate frequency (fig. 9) beginning east of Silverton and continuing to upstream of Eureka. This difference suggests that shallow valley fill sediment is not the sole source of high conductivities. The bedrock is likely more weathered and fractured along the Animas River part of the Silverton caldera structural margins. Another line of evidence that the valley fill is not thick is that the magnetic field map (pl. 3) does not have a pronounced magnetic low along the river basin. A magnetic low would be indicative of thick nonmagnetic sediment.

The CSR map for the lowest frequency is given in figure 10. The apparent conductivity for this frequency is 10 times lower than that for the intermediate frequency shown in figure 9. Apparent conductivity anomalies in this map are smoother than the next higher frequency because again there is greater averaging of the signature of subsurface electrical features. The depth of penetration at the lowest frequency is on the order of 40–50 m. Again there is greater correlation of high apparent conductivities along the upper Animas River drainage than other drainages in the study area. This is likely due to alteration of bedrock along the caldera ring fractures that form the southeastern margin of the Silverton caldera. It is interesting that this is the only part of the caldera structure that has an electrical signature. This suggests that clay minerals are not a large part of the altered rocks along other areas of the caldera margin.

Apparent Conductivity Features

Conductivity anomaly 1 (fig. 11) is an apparent conductivity high with a low at the center. The apparent conductivity high is one of the highest in the survey. The anomaly is prominent in the mid and low frequencies (figs. 9 and 10), suggesting that the surface expression may not be obvious. The general shape is suggestive of an alteration halo around a buried intrusive. The high conductivity (red colors) is situated in an area of moderately high (yellows) apparent conductivity located to the north of linear feature A. This linear feature trends northwest to southeast and correlates well with a fault zone shown by Yager and Bove (2002; Yager and Bove, this volume, pl. 1). In one interpretation of this setting, a silicified fault zone is present that has acted as a barrier to hydrothermal waters. The impounded hydrothermal waters could have caused alteration to the northeast of the structure (D.J. Bove, oral commun., 2002). A high apparent conductivity is correlated with this alteration. This structural zone may also control modern ground-water flow (Wright, Kimball, and Runkel, this volume, Chapter E23).

Linear feature B has a similar trend to linear feature A and passes through the area of the May Day mine (MA, fig. 11). The feature is present on the intermediate- and low-frequency apparent conductivity maps (figs. 9 and 10). That these trends are not as clear on the high-frequency map suggests that the surface expression may not be obvious. This may be why surface geologic maps (Yager and Bove, 2002; Yager and Bove, this volume, pl. 1) do not indicate a prominent structure in this area. Smith and others (2001) suggested that linear feature B may be a fracture system that could control the ground-water flow. Local surficial ground-water flow interaction with the May Day mine dump is also documented (Smith and others, 2001; Wright, Kimball, and Runkel, this volume). Thus this area may be a good example of both surface (mine waste) and subsurface (fracture controlled) ground-water paths. Linear features C and D may indicate similar structures extending to the northwest from linear feature B. These trends are also not as clear on the high-frequency apparent conductivity map (fig. 8).

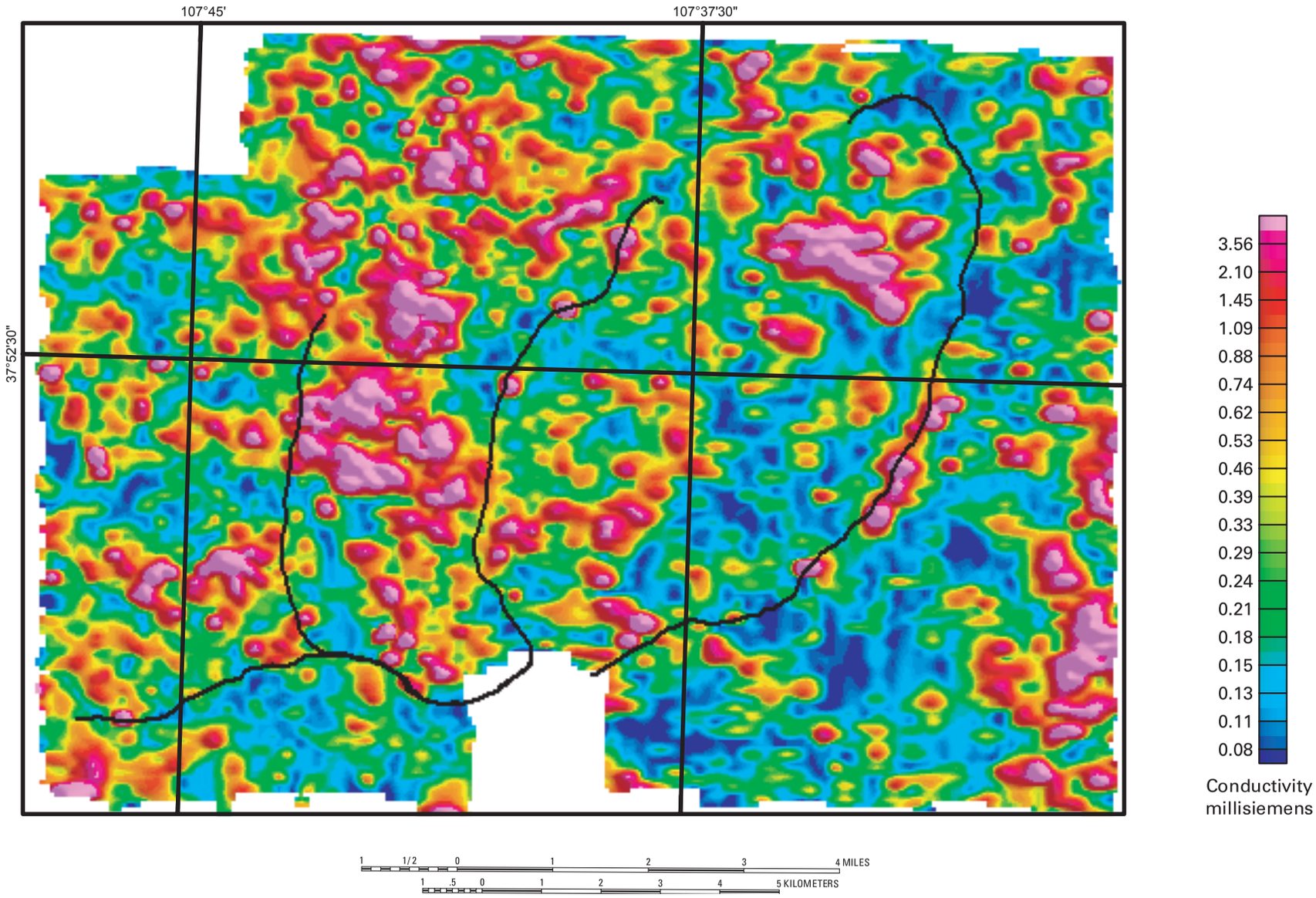

Figure 8. Color shaded-relief apparent conductivity map at 36,930 Hz of Animas River watershed study area. Sun direction is from northeast. Black line, flightline flown along selected drainage as shown in figure 3. Figure is of same area as shown in the 1:48,000 apparent conductivity map (pl. 4).

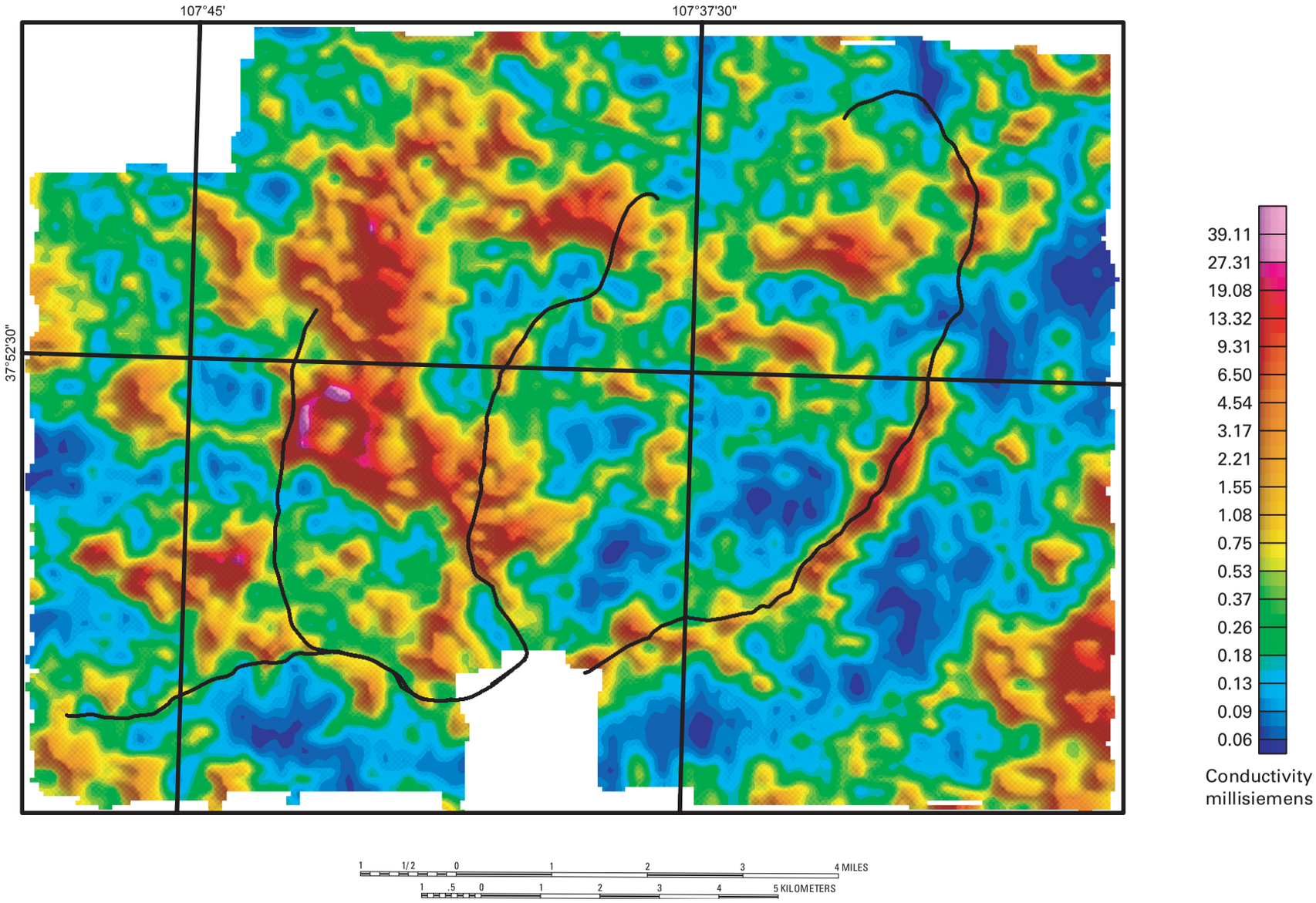

Figure 9. Color shaded-relief apparent conductivity map at 4,310 Hz of Animas River watershed study area. Black line, flightline flown along selected drainage as shown in figure 3. Figure is of same area as shown in the 1:48,000 apparent conductivity map (pl. 4).

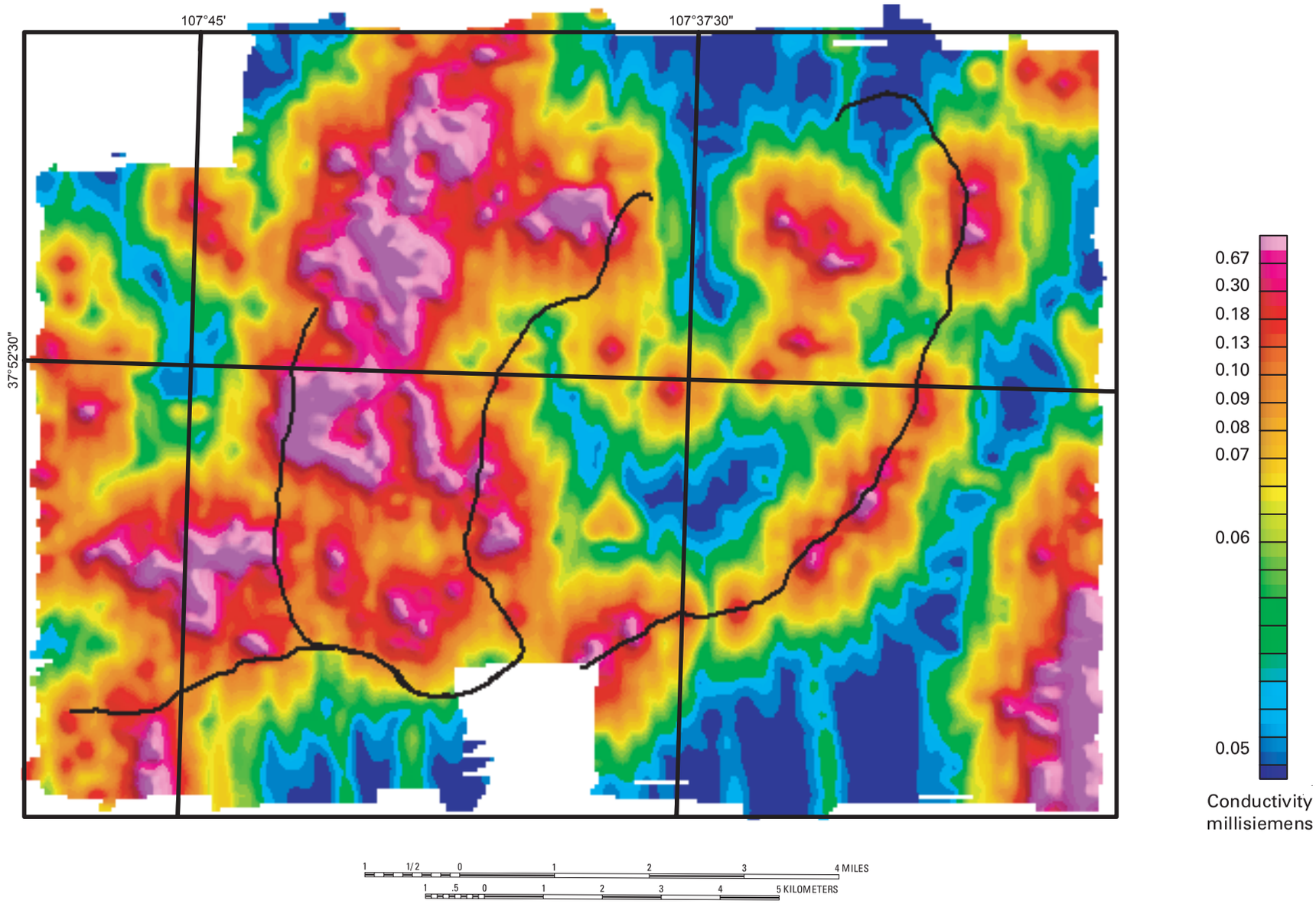

Figure 10. Color shaded-relief apparent conductivity map at 935 Hz of Animas River watershed study area. Black line, flightline flown along selected drainage as shown in figure 3. Figure is of same area as shown in the 1:48,000 apparent conductivity map (pl. 4).

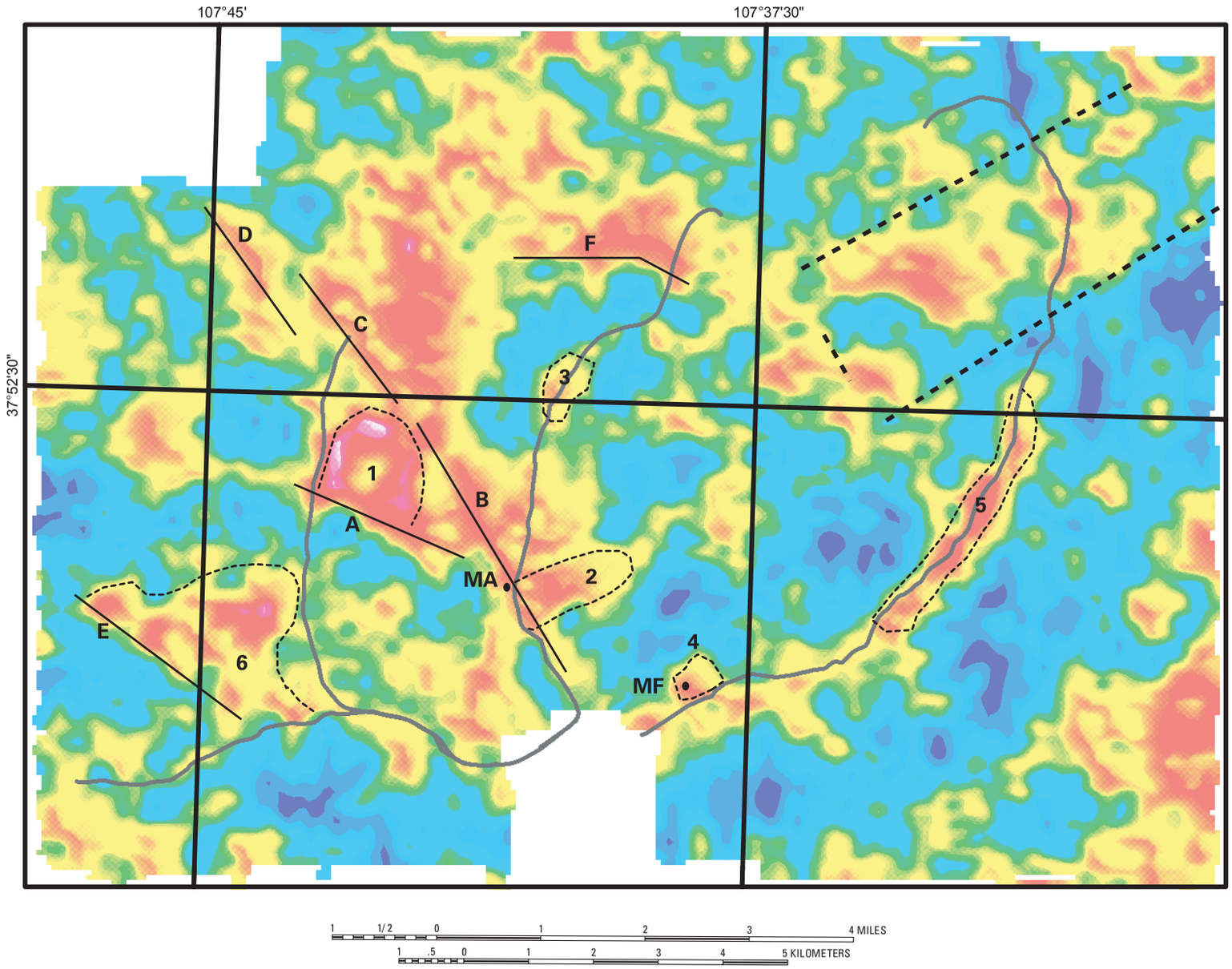

Figure 11. Apparent conductivity map showing selected anomalous features. Curving solid gray line, flightline flown along selected drainage as shown in figure 3. Figure is same area as shown in the 1:48,000 apparent conductivity map with the same color scale (pl. 4). Letters identify linear features (straight black lines); MA, May Day mine; MF; Mayflower tailings. Numbers indicate high conductivity anomalies.

High apparent conductivities located in the area labeled 2 in fig. 11 correlate with a mapped landslide (Yager and Bove, 2002; Yager and Bove, this volume, pl. 1). The high apparent conductivity is present at all frequencies, which suggests that the source extends from surface to depth. Clay minerals, associated with alteration of the Silverton Volcanics, are likely the source of the anomalous conductivity. The clay-rich lithology is favorable for the development of landslides and may also control local ground-water flow.

Anomaly 3, located along Cement Creek, is in the area where an iron-rich bog described in several other studies (Wirt and others, this volume; Kimball and others, this volume; Stanton, Yager, and others, this volume, Chapter E14) has formed. This high conductivity anomaly has an expression at the lower frequency and a very limited expression at the highest frequency. One hypothesis concerning the genesis of the bog is that it could be located on a fracture system that is acting to focus the flow of ground water. The electrical signature is not suggestive of a linear fracture system. In addition, ground electrical geophysical surveys on the bog surface do not indicate any depth extent to the high dissolved solids observed at the surface. The localized conductivity high is due to downcutting of the valley in this part of Cement Creek that has forced ground water to the surface (Vincent and others, this volume, Chapter E16).

Linear feature F (fig. 11), located at the head of Cement Creek, is defined as a boundary between low and high apparent conductivities. The general trend of linear feature F correlates with the Bonita fault and the western part of the Sunnyside fault (Yager and Bove, 2002; Yager and Bove, this volume, pl. 1). The specific location of this linear feature may indicate a part of the fault system that is important in controlling local ground-water flow.

High conductivity anomaly 4 (fig. 11) along the Animas River is located at the Mayflower Mill mine-waste piles (MF) and adjacent flood plain along the river. Ground geophysical surveys in the flood plain along this part of the drainage in 2001 showed localized shallow-subsurface very high conductivity between the waste piles and the Animas River. This high conductivity was correlated with sulfide tailings that were removed in 2003 by Sunnyside Gold, Inc. The high conductivity anomaly, in general, is likely to have resulted from the high dissolved solids in ground water and the presence of conductive sediment in tailings. There is also a large fault zone exposed in the bank of the Animas River that may be the source of some of the high conductivity on the south side of the river east of anomaly 4.

High conductivities are associated with much of the Animas River northeast of Silverton. Conductive anomaly 5 is present on all frequencies (figs. 8, 9, and 10). The source of high conductivities is likely both valley fill and altered bedrock along the valley. The extension of the conductive features to depth could be an indication of structures bounding this part of the Silverton caldera. As a point of interest, note that other major drainages (Mineral Creek, South Fork Mineral Creek, Cement Creek) do not have as extensive areas of high conductivity, even though there is fill along their valleys. The implication is that the ring fault structure is more developed and altered with depth along the Animas River drainage than in the other drainages. Thus both surficial and fracture-controlled ground-water flow is particularly important along this drainage.

Conductivity anomaly 6 and linear feature E (fig. 11) are correlated with the mineralized system at peak 3,792 m (Yager and Bove, this volume; Bove and others, this volume). The high conductivity anomaly is correlated in general with mapped quartz-sericite-pyrite lithology. No single mapped structural feature correlates with linear feature E southwest of this mineralized system (fig. 11).

Hydrologic Implications

Variations in electrical conductivity can be generalized for different types of ground-water systems for the Animas River watershed study area. Water-bearing units in the study area can be conceptually grouped as (1) near surface, (2) weathered surficial bedrock, and (3) deeper bedrock. Ground-water flow within water-bearing units can be associated with and influenced by lithologic and structural heterogeneities that can have contrasting physical properties (electrical conductivity and magnetization). These contrasts in physical properties are shown by the heterogeneous responses in the airborne geophysical maps. Predicting subsurface ground-water flow is important in understanding the transport of contaminants from historical mine sites.

Ground-water flow exists in the Holocene and Pleistocene deposits of clay to boulder-size sediments that are mapped as alluvium, alluvial fans, talus slopes, colluvium, landslides, glacial deposits, and bog deposits (Blair and others, 2002; Yager and Bove, 2002; Yager and Bove, this volume). Areas of silt-size sediment may contain clay minerals that cause a high electrical conductivity. These areas may be associated with alluvium, colluvium, and landslides. Alluvial valley fill may also contain organics (peat type deposits) that can increase the electrical conductivity. Talus slopes and gravel deposits without either clay or water containing high dissolved solids will have low electrical conductivity or be resistive. Rock glaciers that consist of ice cores with sand and boulders are likely to be areas of very high electrical resistivity (very low conductivity). The magnetization of most of the surficial deposits is low except where sediment was derived in place from magnetic bedrock.

The Silverton Volcanics of the Animas River watershed study area are described by Yager and Bove (this volume) as consisting of a basal unit (Burns Member), an overlying (but locally interfingering) pyroxene andesite member, and the Henson Member. The older Burns Member of altered lavas and tuffs has the highest silica content and occupies the central part of the Silverton caldera. The corresponding magnetic low and moderated apparent conductivities are consistent with this lithology, although NRM and hydrothermal alteration may

play a role in causing the low magnetic anomalies. The youngest Henson Member consists of interfingering volcaniclastics that are marked by relatively high magnetic anomalies and low conductivities (high resistivity). Magnetic highs at the south side of the Silverton caldera and just north of the Animas River are correlated with the topographic highs (ridge crests) that are mapped as Henson Member (Lipman and others, 1973).

As noted in the discussion of the apparent resistivities at different frequencies, a progression occurs from higher conductivities at the highest frequency (shallowest penetration) to lower conductivity at the lower frequencies (greatest penetration). Near-surface crystalline bedrock has permeability attributed to a three-dimensional volume of intense fracturing (Hurr and Richards, 1974; Caine and Tomusiak, 2003). Conceptually for the study area, in this zone of weathered and intensely fractured bedrock, seasonal fluctuations of recharge and discharge take place (Caine, 2003). High electrical conductivities may be developed if the ground water contains high dissolved solids characteristic of many contaminants. Weathering processes may also lead to the development of secondary minerals, in particular clay or zeolite minerals. Both of these conditions will contribute to near-surface high conductivities underlain by low conductivity bedrock. An electromagnetic anomalous signature of this setting would be high conductivities at high frequencies and lower conductivities at the deeper penetrating lower frequencies (fig. 10). A contributing factor to the decreasing conductivity with depth is, conceptually, the decreasing fracturing with depth. As lithostatic pressures increase, open fractures should decrease.

Porosity and permeability of volcanic rocks can be associated with primary depositional features and fractures developed at various scales. Bedrock ground-water flow may exist in highly permeable volcanic rock such as tuffs and breccias. There have been no systematic laboratory or borehole measurements of porosity and permeability of the volcanic rocks in the study area. Huntley (1979) and Caine (2003) have suggested that the San Juan Mountains in general have high permeability due to both fracturing and their lithology (tuffs and breccias, for example). Primary deposition features are the extensive lahars, volcaniclastic deposits, and interbedding between flows. The electrical conductivity of porous and permeable sediments is directly controlled by the conductivity of the pore fluid (Olhoeft, 1985). Consequently, large areas (tens of meters) containing fluids with high total dissolved solids can produce high conductivity signatures in the HEM data.

Caine and others (1996) described a conceptual model of the controls of ground-water flow by faults and fault zones. Faults and fractures within aquifers and water-bearing rocks can act as both conduits and barriers to water flow (Caine and others, 1996). Robinson (1978) and Caine and Tomusiak (2003) have given good descriptions of the hydrologic setting of crystalline rock in terms of the importance of faults and fractures. On the scale of geologic time, fault zones and fractures have certainly served as conduits that have focused hydrothermal fluids to form mineral deposits (Casadevall and Ohmoto, 1977). The same hydrothermal processes that have developed and concentrated mineralization also developed extensive siliceous vein systems that have essentially annealed or plugged the fracture system that existed at the time. Massive siliceous vein systems are likely to have low electrical conductivity (be resistive) (Olhoeft, 1985). Unless these are fractured, they are likely barriers to ground-water flow. In contrast, high conductivity may be due to development of clay in tabular alteration zones along faults that act as conduits.

Evidence for specific ground-water flow paths in the watershed is limited and is summarized as follows. The geophysical features extending from the May Day mine toward Ohio Peak (figs. 7 and 11) suggest a structure that influences ground-water flow over a broad scale (Smith and others, 2001). Arcuate magnetic and conductive features that predominantly follow the Animas River suggest that the ring fracture system (Yager and Bove, this volume) influences ground-water flow. Wirt and others (this volume) suggest that development of bogs or precipitates near Fairview and Placer Gulches (middle part of Cement Creek, pls. 3 and 4) is partly due to fracture system-controlled springs. Neither area is near identified linear geophysical anomalies, but both are near anomalous electrical conductivity lows in the intermediate and low electromagnetic frequencies (figs. 9 and 10). The high conductivity anomaly near the Mayflower mine-waste piles is in part associated with a localized flow path that transported high metals from a sulfide-rich mine waste that has been removed. Thus in general the airborne geophysical surveys can be used in the study of both large- and small-scale ground-water flow paths.

Conclusions

The airborne electromagnetic and magnetic maps for the Animas River watershed study area contain features that selectively emphasize specific lithology and structure and offer clues in understanding the ground-water flow regime. The lithology of the caldera fill is associated with magnetic lows and conductivity highs. Younger intrusives ringing the caldera have distinctive geophysical anomalies reflecting differing lithologies.

The geologic maps of the study area show numerous structures, but only a few of these are associated with identified geophysical anomalies. Conversely, data on the geophysical maps suggest structures that have not been previously mapped. Geophysical maps identify areas of near-surface and subsurface electrical and magnetic physical property contrasts that suggest structural features. These structures possibly influence ground-water flow.

Electrical and magnetic signatures can be associated with particular lithologies. Only qualitative relationships have been suggested here. McDougal and others (this volume) have used predictive models to quantitatively relate geophysical signatures to acid-neutralizing terrains and terrains favorable for the occurrence of veins and structures. Physical property

differences between Tertiary intrusives enable them to be classified on the basis of their geophysical signature. Low conductivity and magnetic intrusives may have more restricted ground-water flow than those that have been altered producing magnetic lows and a conductive signature.

Near-surface high conductivity anomalies associated with some mine-waste piles may indicate ground water containing high dissolved solids or a source of metal loading to the ground water. Other areas of intense hydrothermal alteration may be a surface source for ground water containing high dissolved solids.

The geophysical data have been used to identify areas possibly influencing surface and bedrock ground-water flow. Location of subsurface ground-water flow paths is a critical part of abandoned mine land studies.

References Cited

Aero Service Corp., 1979, Airborne gamma-ray spectrometer and magnetometer survey, Durango quadrangle, Colorado: U.S. Department of Energy, Grand Junction Office Report GJBX–143 (79), 2 volumes.

Blair, R.W., Jr., Yager, D.B., and Church, S.E., 2002, Surficial geologic maps along the riparian zone of the Animas River and its headwater tributaries, Silverton to Durango, Colorado, with upper Animas River watershed gradient profiles: U.S. Geological Survey Digital Data Series 071.

Bove, D.J., Hon, Ken, Buddington, K.E., Slack, J.F., and Snee, L.W., 2001, Geochronology and geology of late Oligocene through Miocene volcanism and mineralization in the western San Juan Mountains, Colorado: U.S. Geological Survey Professional Paper 1642, 30 p.

Bove, D.J., Mast, M.A., Wright, W.G., Verplanck, P.L., Meeker, G.P., and Yager, D.B., 2000, Geologic controls on acidic and metal-rich waters in the southeast Red Mountain area, near Silverton, Colorado, *in* ICARD 2000; Proceedings of the Fifth International Conference on Acid Rock Drainage, Volume 1: Society for Mining, Metallurgy, and Exploration Inc., p. 523–533.

Burbank, W.S., and Luedke, R.G., 1969, Geology and ore deposits of the Eureka and adjoining districts, San Juan Mountains, Colorado: U.S. Geological Survey Professional Paper 535, 73 p.

Caine, J.S., 2003, Characterizing groundwater hydrology in high gradient terrains underlain by complex geology; focus on the San Juan Mountains of southwestern Colorado: Rocky Mountain Section of the Geological Society of America, 55th Annual Meeting, Abstracts with Programs, v. 35, no. 5, p. 5–6.

Caine, J.S., Evans, J.P., and Forster, C.B., 1996, Fault zone architecture and permeability structure: Geology, v. 24, p. 1025–1028.

Caine, J.S., and Tomusiak, R.A., 2003, Brittle structures and their role in controlling porosity and permeability in a complex Precambrian crystalline-rock aquifer system in the Colorado Rocky Mountain Front Range: Geological Society of America Bulletin, v. 115, no. 11, p. 1410–1424.

Casadevall, Thomas, and Ohmoto, Hiroshi, 1977, Sunnyside mine, Eureka mining district, San Juan County, Colorado—Geochemistry of gold and base metal ore deposition in a volcanic environment: Economic Geology, v. 92, p. 1285–1320.

Fitterman, D.V., 1999, Sources of calibration errors in Helicopter EM data: Exploration Geophysics, Australian Society of Exploration Geophysicists, v. 29, p. 65–70.

Fraser, D., 1978, Resistivity mapping with an airborne multicoil electromagnetic system: Geophysics, v. 43, p. 144–172.

Grauch, V.J.S., 1987a, Interpretive aeromagnetic map using the horizontal gradient; Lake City caldera area, San Juan Mountains, Colorado: U.S. Geological Survey Geophysical Investigations Map GP–974, scale 1:48,000.

Grauch, V.J.S., 1987b, A new variable-magnetization terrain correction method for aeromagnetic data: Geophysics, v. 52, p. 94–107.

Grauch, V.J.S., and Hudson, M.R., 1987, Summary of natural remanent magnetization, magnetic susceptibility, and density measurements from the Lake City caldera area, San Juan Mountains, Colorado: U.S. Geological Survey Open-File Report 87–182, 23 p.

Gettings, M.E., Fisher, F.S., Gettings, P.E., and Luedke, R.G., 1994, Some magnetic properties of rocks from the Silverton caldera area, Western San Juan Mountains, Colorado: U.S. Geological Survey Open-File Report 94–291, 28 p.

High Life Helicopters, Inc., 1981, Contour maps of uranium, uranium/thorium ratio and total field magnetics, Lake City Area, San Juan Mountains, Colorado: U.S. Geological Survey Open-File Report 81–567, 7 p.

High Life Helicopters, Inc., 1983, Airborne gamma-ray spectrometer and magnetometer survey, Durango A, B, C, and D, Colorado detail areas: U.S. Department of Energy Report GJBX–031(83).

Huntley, D., 1979, Ground-water recharge to the aquifers of northern San Luis Valley, Colorado: Geological Society of America Bulletin, Part II, v. 90, no. 8, p. 1196–1281.

Hurr, R.T., and Richards, D.B., 1974, Hydrologic investigations, *in* Robinson, C.S., and others, Engineering, geologic, geophysical, hydrologic, and rock mechanics investigations of the Straight Creek Tunnel site and pilot bore, Colorado: U.S. Geological Survey Professional Paper 815, p. 79–88.

Lipman, P.W., Steven, T.A., Luedke, R.G., and Burbank, W.S., 1973, Revised volcanic history of the San Juan, Uncompahgre, Silverton and Lake City calderas in the western San Juan Mountains, Colorado: U.S. Geological Survey Journal of Research, v. 1, p. 627–642.

McCafferty, A.E., Van Gosen, B.S., Smith, B.D., and Sole, T.C., 2004, Geophysical characterization of geologic features with environmental implications from airborne magnetic and apparent resistivity data, Chapter D2 *in* Nimick, D.A., Church, S.E., and Finger, S.E., eds., Integrated investigations of environmental effects of historical mining in the Basin and Boulder mining districts, Boulder River watershed, Jefferson County Montana: U.S. Geological Survey Professional Paper 1652, p. 89–126.

Olhoeft, G.R., 1985, Low-frequency electrical properties: Geophysics, v. 50, no. 12, p. 2492–2503.

Oshetski, K.C., and Kucks, R.P., 2000, Colorado aeromagnetic and gravity maps and data; A Web site for distribution of data (on-line version): U.S. Geological Survey Open-File Report 00–0042, 12 p. Available at URL http://pubs.usgs.gov/of/2000/ofr-00-042/colorado.htm.

Phillips, J.D., 1997, Potential-field geophysical software for the PC, version 2.2: U.S. Geological Survey Open-File Report 97–725, 34 p.

Phillips, J.D., Duvall, J.S., and Saltus, R.W., 2003, Geosoft eXecutables (GX's) developed by the U.S. Geological Survey, version 1.0, with a viewgraph tutorial on GX development: U.S. Geological Survey Open-File Report 03–010, 23 p.

Robinson, C.S., 1978, Hydrology of fractured crystalline rocks, Henderson mine, Colorado: Mining Engineering, v. 28, p. 1185–1195.

Smith, B.D., Campbell, D.L., and Wright, W.G., 2001, Using resistivity to map acidic waters at the May Day mine dump, Silverton, Colorado: Proceedings for the Symposium on the Application of Geophysics to Environmental and Engineering Problems, Denver, Colo., March 4–7, 14 p.

Smith, B.D., McCafferty, A.E., and McDougal, R.R., 2000, Utilization of airborne magnetic, electromagnetic, and radiometric data in abandoned mine land investigations, *in* ICARD 2000; Proceedings of the Fifth International Conference on Acid Rock Drainage, Volume 2: Society for Mining, Metallurgy, and Exploration, Inc., p. 1524–1538.

Smith, B.D., McDougal, R.R., McCafferty, A.E., Deszcz-Pan, Maryla, and Yager, D.B., 2004, Helicopter electromagnetic and magnetic survey of the upper Animas River watershed; application to abandoned mine land studies: Proceedings for the Symposium on the Application of Geophysics to Environmental and Engineering Problems, Colorado Springs, Colo., February 22–26, 16 p.

Syberg, F.J.R., 1972, A Fourier method for the regional-residual problem of potential fields: Geophysical Prospecting, v. 20, p. 47–75.

Telford, W.M., Geldart, L.P., and Sheriff, R.E., 1978, Applied geophysics, First Edition: Cambridge, England, Cambridge University Press, 561 p.

Yager, D.B., and Bove, D.J., 2002, Generalized geologic map of part of the upper Animas River watershed and vicinity, Silverton, Colorado: U.S. Geological Survey Miscellaneous Field Studies Map MF–2377, scale 1:48,000.